Accepted refereed manuscript of: Garrido D, Monroig O, Galindo A, Betancor M, Perez JA, Kabeya N, Marrero M & Rodriguez C (2020) Lipid metabolism in Tinca tinca and its n-3 LC-PUFA biosynthesis capacity. *Aquaculture*, 523, Art. No.: 735147.DOI: https://doi.org/10.1016/j.aquaculture.2020.735147

Lipid metabolism in *Tinca tinca* and its n3 LC-PUFA biosynthesis capacity

D. Garrido[1], Ó. Monroig[2,3], A. Galindo[1], M.B. Betancor[2], J.A. Pérez[1], N. Kabeya[2,4], M. Marrero[1], C. Rodríguez[1]

[1]Departamento de Biología Animal, Edafología y Geología, Universidad de La Laguna, La Laguna 38206, Santa Cruz de Tenerife, Spain.

[2]Institute of Aquaculture, Faculty of Natural Sciences, University of Stirling, Stirling FK9 4LA, Scotland, UK.

[3]Instituto de Acuicultura Torre de la Sal, Consejo Superior de Investigaciones Científicas (IATS-CSIC), 12595 Ribera de Cabanes, Castellón, Spain.

[4]Department of Aquatic Bioscience, The University of Tokyo, Yayoi, Bunkyo-ku, Tokyo, Japan

*Corresponding author: Covadonga Rodríguez González

Mailing address: covarodr@ull.edu.es

Tel.: +34922316502 (Ext. 6574)

e-mail: covarodr@ull.edu.es

Abbreviations

AA: arachidonic acid; AdA: adrenic acid; ALA: linolenic acid; BHT: butylated hydroxyl toluene; cDNA: complementary DNA; DGLA: dihomo-γ-linolenic acid; DHA: docosahexaenoic acid; DPA: docosapentaenoic acid; EDA: eicosadienoic acid; ef1α: elongation factor-1α; Elovl2: fatty acyl elongase 2; Elovl5: fatty acyl elongase 5; EPA: eicosapentaenoic acid; ETA: eicosatetraenoic acid; ETE: eicosatrienoic acid; FA: fatty acid; Fads2: fatty acyl desaturase; FAF-BSA: fatty acid free bovine serum albumin; FAME: fatty acid methyl esters; FFA: free fatty acid; GLA: γ-linolenic acid; HBSS: Hanks balanced salt solution; LA: linoleic acid; LC-PUFA: long chain polyunsaturated fatty acid; NTC: negative controls; ORF: open reading fragment; PCA: principal component analysis; PCR: polymerase chain reaction; PUFA: polyunsaturated fatty acid; qPCR: quantification real-time PCR; RACE: rapid amplification of cDNA ends; TL: total lipid**.**

Abstract

Carps, barbels and other cyprinids are the major contributors to freshwater aquaculture at global scale. Nevertheless, freshwater fish aquaculture needs to diversify their production in order to offer consumers new species. Tench (*Tinca tinca*) is a freshwater species with great interest for the diversification of continental aquaculture. However, up to date, no commercial formulated diet exists for this species in order to optimize their nutritional requirements and the quality of its final product. Using multiple methodological approaches, the aim of this study was to evaluate the long chain polyunsaturated fatty acid (LC-PUFA) metabolism of *T. tinca*. Firstly, the molecular cloning and functional characterisation by heterologous expression in yeast of a desaturase (Fads2) and two elongases (Elovl2 and Elovl5) involved in LC-PUFA biosynthesis, and the analysis of gene expression among tissues were performed. Secondly, in order to confirm the LC-PUFA biosynthesis capacity of isolated hepatocytes and enterocytes, cells were incubated with [1-^{14}C] labelled linoleic acid (18:2n-6, LA), linolenic acid (18:3n-3, ALA) and eicosapentaenoic acid (20:5n-3, EPA). In yeast, Fads2 showed a Δ6/Δ5 bifunctional activity. Elovl2 was more active over C_{20} and C_{22} substrates, whereas Elovl5 was over C_{18} and C_{20}. Liver displayed the highest expression for the three target genes (*fads2, elovl2* and *elovl5*). Incubated cells also showed Fads2 bifunctional activity as well as elongation products in concordance with yeast heterologous expression results. Importantly, our results demonstrated that tench is able to biosynthesise docosahexaenoic acid (DHA) from 18:3n-3 in both hepatocytes and enterocytes, a capacity that seems to explain in part the surprisingly high levels of DHA found in the fish flesh compared to its dietary supply. Tench is a promising freshwater species with a potential capacity to endogenously increase its

flesh DHA contents, reducing the impact that the usage of fish oils from forage fisheries may have on the aquaculture industry.

Keywords

Biosynthesis, fatty acyl desaturase, fatty acyl elongase, long-chain polyunsaturated fatty acid, radiolabelled fatty acid, *Tinca tinca*

1. Introduction

The challenge of producing food for 9 billion people by 2050 means that current food production needs to double (Béné et al., 2015). Nowadays, fisheries and aquaculture supply among 50% and 60% per capita intake of animal protein in some areas of Africa and Asia, respectively (de Roos et al., 2017). However, the overexploitation of fisheries and the use of their captures to produce aquafeeds compromise the environmental and economic sustainability of aquaculture to meet future demands for animal protein. Different strategies have been considered in aquaculture research to solve the aforementioned challenge including dietary fish meal and fish oil replacement by terrestrial sources as well as the diversification of aquaculture with fish from different trophic levels likely to have lower lipid requirements and n3 long chain polyunsaturated fatty acid (LC-PUFA; ≥20 carbon atoms and ≥three double bonds) biosynthesis capacities (Castro et al., 2016; Garrido et al., 2019; Tocher, 2015).

Freshwater species represent the largest contribution to the global aquaculture fish production, with a 94.9% in 2017 (FAO Fisheries and Aquaculture Department, 2017). China is the greatest producer (90.4%), followed by America, Africa and Europe with 2.1%, 1.8% and 0.6%, respectively. Carps, barbels and other cyprinids are the major contributors to freshwater aquaculture. Nevertheless, freshwater fish aquaculture needs to diversify their production in order to offer consumers new species.

The cyprinidae tench (*Tinca tinca* Linnaeus, 1758) has been identified as a promising species for the diversification of the freshwater aquaculture industry (Celada et al., 2009). Native to parts of Europe and Siberia, it has been successfully introduced in Chile, USA, Africa, India, Korea, China, Australia, and New Zealand (Pula et al., 2018; Wang et al., 2006) mainly due to its flesh quality, high market price and interest

for recreational angler activity (Ljubojević et al., 2014; Vinatea et al., 2018; Wang et al., 2006; Wolnicki et al., 2006). Considering the ability of tench to live in high turbidity and low oxygen environments, its versatility to be farmed in different systems and conditions, its resistance to viral diseases, feeding plasticity, successful response to spawning induction at only 1 year old, wide spawning seasons and long lifespan, it is surprising that its culture has not risen up as other cyprinids (González-Rodríguez et al., 2014; Ljubojević et al., 2014; Panicz, 2016; Panicz et al., 2017; Rodríguez et al., 2004; Wang et al., 2006). Its slow growth in captivity, probably associated to the lack of a balanced commercial diet, is partly responsible for its stagnant global production between 2500-3200 ton per year since 2013 (FAO Fisheries and Aquaculture Department, 2017). Therefore, one of the main bottlenecks to be solved in order to foster culture of tench relays on the improvement of the knowledge on the nutritional requirements of this species, including lipids (Celada et al., 2009; García et al., 2015; Ljubojević et al., 2014; Panicz et al., 2017). In this sense, feedstuffs with high lipid content used for other freshwater fish seem to be associated with high deformity ratios in tench (Celada et al., 2009; Pula et al., 2018; Wolnicki et al., 2006). In addition, the n3 LC-PUFA content in flesh, has been reported to be influenced by dietary fatty acid composition since it can affect fish n3 LC-PUFA biosynthetic capacity (Ljubojević et al., 2014). LC-PUFA biosynthetic pathways involve the action of both fatty acyl desaturases (Fads) and elongases of very long-chain fatty acids (Elovl) (Fig. 1). Fads insert a double bond between a pre-existent one and the carboxylic group, and are also known as “front-end” desaturases. Moreover, Elovl are rate-limiting enzymes involved in the pathway of elongation of fatty acids (Castro et al., 2016).

Cyprinidae such as common carp (*Cyprinus carpio)* and zebrafish (*Danio rerio*) have been demonstrated to possess fatty acyl desaturases 2 (Fads2) with dual Δ6 and Δ5

desaturase activities (Hastings et al., 2001; Zheng et al., 2004). Moreover, the zebrafish Fads2 was further confirmed to have Δ6 activity over C_{24} substrates as well as a Δ8 activity (Monroig et al., 2011; Oboh et al., 2017; Tocher et al., 2003). Two Fads2 have also been reported in *C. carpio*, although they still remain functionally uncharacterised (Ren et al., 2012). More than one Fads2 has been found in the freshwater fish pike silverside (*Chirostoma estor*), striped snakehead (*Channa striata*), and Nile tilapia (*Oreochromis niloticus*) (Fonseca-Madrigal et al., 2014; Kuah et al., 2016; Oboh et al., 2017; Tanomman et al., 2013), anadromous Atlantic salmon *Salmo salar* (Monroig et al., 2010b), and rabbitfish (*Siganus canaliculatus*) (Li et al., 2010) as a possible result of gene duplication (Monroig et al., 2010b).

Elongases Elovl2, Elovl4 and Elovl5 required for the biosynthesis of LC-PUFA have been found in zebrafish (Agaba et al., 2005; Jakobsson et al., 2006; Monroig et al., 2009, 2010a). Elovl5 has a preferential elongation activity over C_{18} and C_{20} substrates (Agaba et al., 2005) whereas Elovl2 has C_{20} and C_{22} PUFA as preferred substrates (Monroig et al., 2009). Two Elovl4 described in zebrafish (*D. rerio*) are able to elongate C_{20} substrates such as eicosapentaenoic acid (20:5n-3, EPA) and arachidonic acid (20:4n-6, AA) to produce up to C_{36} fatty acids, with Elovl4b being involved in the elongation step previous to desaturation and chain shortening to produce docosahexaenoic acid (22:6n-3, DHA; Monroig et al., 2010a). In *C. carpio* the molecular characterisation of an Elovl5 has been also reported (Ren et al., 2012).

Ljubojević et al. (2014) suggested that tench had some desaturase and elongase capacity since they were able to detect γ-linolenic acid (18:3n-6, GLA), dihomo-γ-linolenic acid (20:3n-6, DGLA), eicosadienoic acid (20:2n-6, EDA) and eicosatrienoic acid (20:3n-3 ETE) in muscle of fish fed diets lacking those fatty acids. However, the complement and function of genes encoding desaturase and elongase enzymes

accounting for such conversions remains unknown. The present study aimed to elucidate the molecular cloning, functional characterisation and tissue distribution of *fads2*, *elovl2* and *elovl5*, genes involved in the biosynthesis of n3 LC-PUFA in tench (*Tinca tinca*). Moreover, the metabolic pathways involved in the biosynthesis of LC-PUFA in isolated enterocytes and hepatocytes were investigated through metabolic monitoring of radiolabelled fatty acid substrates.

2. Material and methods

This study was carried out according to Spanish law 6/2013 based on the European Union directive on animal welfare (Directive 2010/63/EU) on the protection of animals used for scientific purposes and authorized by the Ethics Committee at the University of La Laguna.

2.1. Fish rearing

A total of five male tench juveniles of 388.2 ± 79.6 g average final weight were used in the present study. The specimens were cultured from fry stages at the facilities of "Centro de Acuicultura Vegas del Guadiana" (Badajoz, Spain) in a 1.500 m^3 pond under natural photoperiod and thermoperiod from May 2015 to November 2016. Fish were fed the last 9 months previous to tissue collection with a cyprinid commercial diet manufactured by Dibaq (Segovia, Spain) which lipid and fatty acid composition is given in Table 1.

2.2 Tissue collection

Fish were starved for 24h prior to their transport to the Department of Chemistry "Profesor Carlos Vilchez Martín" (University of Huelva, Spain) where they were sacrificed. Fish were slaughtered by a percussive blow to the head and 50-100 mg samples of muscle, liver, heart, spleen, foregut (from here onwards referred to as gut), brain and gills were collected for molecular cloning, functional characterisation and gene expression tissue distribution. Samples were immediately stored into RNA*later* (Qiagen Iberia, S.L., Madrid, Spain), the first 24h at 4°C and then frozen at -20°C until further analysis. Both lipid determinations and *in vitro* metabolism studies using [1-^{14}C]

fatty acids were carried out on fresh isolated enterocytes and hepatocytes as described in detail in section 2.8.

2.3. Molecular cloning of *fads2, elovl2* and *elovl5* cDNAs

Total RNA was extracted from each tissue using TRI Reagent (Sigma-Aldrich, Dorset, UK) according to manufacturer's instructions and using a bead tissue disruptor (Bio Spec, Bartlesville, Oklahoma, USA). Then, strand cDNA was synthesised from 2 µg of total RNA (mixture from brain and liver (1:1)) using a High Capacity cDNA Reverse Transcription Kits (AB Applied Byosystems, California, USA). In order to obtain the first fragments of *fads2, elovl2* and *elovl5* genes by polymerase chain reaction (PCR) the cDNA was used as template together with degenerated primers (Table 2) and GoTaq® Green Master Mix (Promega, Southampton, UK). The degenerated primers for *fads2*, *elovl2* and *elovl5* were designed on conserved regions from sequences obtained from NCBI blastn tool (http://www.ncbi.nlm.nih.gov/) of several teleost species. For *fads2*, the sequence of *Gadus morhua* (DQ054840.2), *Solea senegalensis* (JN673546.1), *Sparus aurata* (AY055749.1), *Epinephelus coioides* (EU715405.1), *Rachycentron canadum* (FJ440238.1), *Siganus canaliculatus* (EF424276.2), and *Chirostoma estor* (KJ417838.1 and KJ417839.1) were used. For *elovl2*, we selected the sequence of teleosts *Salmo salar* (FJ237532.1), *Clarias gariepinus* (KU902414.1), *Esox lucius* (XM_010885755.3), *Danio rerio* (NM_001040362.1) *Sinocyclocheilus rhinocerous* (XM_016542599.1), whereas for *elovl5*, *S. canaliculatus* (GU597350.1), *E. coioides* (KF006241.1), *R. canadum* (FJ440239.1), *S. senegalensis* (JN793448.1), *C. estor* (KJ417837.1), *S. aurata* (AY660879.1), *S. salar* (NM_001123567.2) were selected. The alignment for each gene was carried out with BioEdit v7.0.9 (Tom Hall, Department of Microbiology, North Carolina State University, USA).

The PCR to amplify the first fragments were performed by an initial denaturing step at 95°C for 2 min, followed by the PCR conditions shown in Table 2 for each primer set, followed by a final extension at 72°C for 5 min. The PCR fragments were purified on agarose gels using Illustra^{TM} GFX^{TM} PCR DNA and Gel Band Purification kit (GE Healthcare Life Sciences, Buckinghamshire, UK) and cloned into pGEM-T Easy vector (Promega, UK) and sequenced (GATC Biotech, Konstanz, Germany). In order to determine 5' and 3' ends of each gene, we subsequently performed Rapid Amplification of cDNA Ends (RACE). The cDNA for RACE were prepared by FirstChoice® RLM-RACE kit (Ambion, Applied Biosystems, Warrington, UK) following manufacturer's recommendations. The first and nested primers for the RACE were designed to anneal to the sequence of the first fragments obtained above (Table 2). All RACE PCR conditions and primers used were also summarised in Table 2. After the nested PCR using the first PCR product as a template, we successfully amplified each cDNA ends fragment of *fads2*, *elovl2* and *elovl5* except 5' end fragment of *fads2*. Therefore, we decided to use *fads2*-like sequence retrieved from their transcriptome assembly (GFZX01031420). All RACE fragments of each gene were sequenced described above and assembled with the corresponding first-fragments to obtain putative full-length cDNA.

2.4. Sequence and phylogenetic analyses

The deduced amino acid (aa) sequences of putative Fads2, Elovl2 and Elovl5 proteins isolated from tench and multiple functionally characterised Fads1, Fads2, Elovl2, Elovl4 and Elovl5 obtained from NCBI were aligned for desaturases or elongases using MAFFT (https://mafft.cbrc.jp/alignment/software/) Ver. 7.388 with the E-INS-i strategy (Katoh et al., 2017). All columns containing gaps in the obtained

alignments were removed by trimAl (Capella-Gutiérrez et al., 2009). The cleaned alignments were subjected to a maximum likelihood phylogenetic analysis using RAxML with 1000 rapid bootstrap replicates. The best-fit evolutionary model was selected to LG+G+I for both genes by ModelTest-NG (Darriba et al., 2019). The resultant RAxML trees were visualised using Interactive Tree Of Life v3 (Letunic and Bork, 2016).

2.5. Functional characterisation

PCR fragments corresponding to the open reading frame (ORF) of *fads2*, *elovl2* and *elovl5* were amplified from a mixture of cDNA (liver and brain) by nested PCR. All primers and PCR conditions were described in Table 2. After the first-round PCR using primer pairs named "ORF cloning first" for each gene, the nested PCR were conducted using first-round PCR product as a template with primer pairs named "ORF cloning nested". The nested primers contain restriction site (underlined in Table 2) to ligate into the yeast expression vector (pYES2). The PCR products were subsequently purified (Illustra GFX PCR DNA/Gel Band Purification kit, GE Healthcare, UK), digested with the corresponding restriction enzymes (Promega, UK) and ligated into a similarly restricted pYES2 yeast expression vector (Invitrogen, Thermo Fisher Scientific, Hemel Hempstead, UK). The potential plasmids containing pYES2-fads2, pYES2-elovl2 and pYES2-elovl5 were purified (GenElute™ Plasmid Miniprep Kit, Sigma, UK) and then used to transform *Saccharomyces cerevisiae* competent cells (*S.c.* EasyComp Transformation Kit, Invitrogen, UK). Transformation and selection of yeast culture were performed as described in Monroig et al. (2018). One single yeast colony transformed of pYES2-fads2, pYES2-elovl2 and pYES2-elovl5 was used in each functional assay. For pYES2-fads2, the transgenic yeasts were grown with one of the

following substrates: LA, ALA, EDA, ETE, DGLA, eicosatetraenoic acid (20:4n-3, ETA), adrenic acid (22:4n-6, AdA) and docosapentaenoic acid (22:5n-3, DPA) while for pYES2-elovl2 and pYES2-elovl5 were grown with 18:2n-6, 18:3n-3, 18:3n-6, 18:4n-3, 20:4n-6, 20:5n-3, 22:4n-6 and 22:5n-3. The fatty acid (FA) substrates were added to the yeast cultures at final concentrations of 0.5 mM C_{18}, 0.75 mM C_{20} and 1.0 mM C_{22} as uptake efficiency decreases with increasing chain length (Lopes-Marques et al., 2017). In addition, yeasts transformed with empty pYES2 were also grown in presence of each substrate as control treatments. After 2 days of culture at 30°C, yeasts were harvested and total lipid extracted by homogenisation in chloroform/methanol (2:1, v/v) containing 0.01% butylated hydroxyl toluene (BHT) as antioxidant.

2.6. Fatty acid analysis of yeast

Fatty acid methyl esters (FAME) were performed from total lipid extracted from yeast according to Hastings et al. (2001). FAME were separated and quantified using a Fisons GC-8160 (Thermo Fisher Scientific, Hemel Hempstead, UK) gas chromatograph equipped with a 60 m x 0.32 mm i.d. x 0.25 µm ZB-wax column (Phenomenex, Macclesfield, UK) and flame ionisation detector (Oboh et al., 2016). The desaturation or elongation conversion efficiencies from exogenously added PUFA substrates were calculated by the proportion of substrate FA converted to desaturated or elongated products as [product area / (product area + substrate area)] × 100.

2.7. Tissue expression of *fads2*, *elovl2* and *elovl5*

Expression of *fads2*, *elovl2* and *elovl5* was determined by relative quantification real-time PCR (qPCR) in muscle, liver, heart, spleen, gut, brain and gill. Replicate numbers were n=4 for each tissue and gene except for *fads2* which were n=3.

Elongation factor-1α (*ef1α*), *β-actin* and 18S were tested as housekeeping genes, being selected *ef1α* and *β-actin* as the most stable genes according to geNorm (M stability value = 0.165; Vandesompele et al., 2002) to assess the expression of *fads2*, *elovl2* and *elovl5* (Table 2). Total RNA was extracted and reverse transcribed using 2 µg of RNA from each tissue. In order to determine the efficiency of the primer pairs, serial dilutions of pooled cDNA were carried out. qPCR was performed on a Biometra TOptical Thermocycler (Analytik Jena, Goettingen, Germany) in 96-well plates in duplicates at total volumes of 20 µL containing 10 µL of Luminaris Color HiGreen qPCR Master Mix (Thermo Scientific, UK), 1 µL of each primer (10 pmol), 2 µL or 5 µL of cDNA (1/20 dilution) for reference and target genes respectively, as well as 6 or 3 µL of molecular biology grade water. Besides, negative controls (NTC, no template control), containing 5 µL molecular biology grade water, instead of template, were also run. The qPCR thermal conditions were 50°C for 2 min, 95°C for 10 min followed by 35 cycles of denaturation, annealing, and extension (details in Table 2). Finally, a melting curve with 1°C increments during 6 s from 60 to 95°C was performed, in order to check the presence of a single product in each reaction. The relative expression of *fads2*, *elovl2* and *elovl5* among tissues was calculated as arbitrary units after normalisation by dividing by the expression level of the geometric mean of the housekeeping genes (*ef1α* and *β-actin*). Arbitrary units were obtained for each target gene (*fads2*, *elovl2*, and *elovl5*) and tissue from the ratio between the expression level of each of them and the tissue with the lowest expression level within these.

2.8. Fatty acid composition and incubation of cells with radiolabelled [1-^{14}C] fatty acids.

Enterocytes and hepatocytes were obtained as described by Rodríguez et al. (2002). The foregut was cleaned of food and faeces and the liver perfused through the hepatic portal vein with a solution of marine Ringer (116 mM NaCl, 6 mM KCl, 1 mM $CaCl_2$, 1 mM $MgSO_4$, 10 mM $NaHCO_3$, 1 mM NaH_2PO_4, 10 mM K_2SO_4 and 10 mM HEPES, at pH 7.4). Tissues were chopped with Hanks Balanced Salt Solution (HBSS) (NaCl 1.75%, 9.69 mM HEPES, 1.73 mM $NaHCO_3$) and incubated with collagenase at 10 mg/mL by gently shaking at 20ºC for 40 min. The resultant cell suspension was filtered through a 100 µm nylon mesh with HBSS containing 1% fatty acid free bovine serum albumin (FAF-BSA). Cells were collected by centrifugation at 716 *g* for 10 minutes, washed with HBSS and re-centrifuged for 7 min. The whole experiment was developed under a cold environment to avoid tissues degradation. After isolation, each cell preparation was incubated for 3h with 0.20 µCi of each radiolabelled [1-^{14}C] PUFA (18:2n-6, 18:3n-3 and 20:5n-3). Besides, a control group of each cell type without radiolabelled FA supplement was also maintained under the same experimental conditions. After incubation, cell viability was assessed by using the trypan blue exclusion test (>90% in all cases). After washing the cells by successive centrifugations to remove remaining radioactivity, the pellets were stored at -80°C until analysis.

Lipid was extracted from isolated cells as described by Christie and Han (2010), while the protein content was determined according to Lowry et al. (1951) using FAF-BSA as standard.

An aliquot of TL (100 µg) of cells incubated with radiolabelled FA was used to determine radioactivity incorporated into TL using a β liquid scintillation counter (TRI-CARB 4810TR, Perkin Elmer, Singapur). Results obtained in dpm (disintegrations per minute) were related to TL and protein content, and transformed to picomoles per mg protein and per hour (pmol/mg prot · h).

To determine the FA elongation/desaturation activities, another aliquot of 0.1 mg of the total lipid (TL) extract from each cell type and radiolabelled FA were transmethylated by acid-catalysis and applied and separated by argentation thin layer chromatography (Rodríguez et al., 2002). The TLC plates were developed in toluene/acetonitrile where 50 µL of a standard with a mixture of the incubated substrates and other radiolabelled FA metabolites was also loaded at the right margin of the plate. The developed plates were then kept into closed Exposure Cassette-K (BioRad, Madrid, Spain) in contact with a radioactive-sensitive phosphorus screen (Image Screen-K, BioRad, Spain) for two weeks. The screens were scanned by an image acquisition system (Molecular Imager FX, BioRad, Spain) and the radioactive products resultant from the metabolic transformation of the FA substrates, were quantified by image analysis software (Quantity One ver. 4.5.2, BioRad, Spain).

TL extracts from cells without radiolabelled FA (control treatment) as well as from fish flesh and diet samples were subjected to acid-catalysed transmethylation, being fatty acid methyl esters purified by thin-layer chromatography (Macherey-Nagel, Düren, Germany), and separated and quantified using a TRACE-GC Ultra gas chromatograph (Thermo Scientific, Milan, Italy) equipped with an on-column injection, a flame ionisation detector (FID) and a fused silica capillary column Supelcowax TM 10 (30 m x 0.32 mm ID) (Supelco Inc., Bellefonte, USA). Helium was used as the carrier gas at 1.5 mL/min constant flow, and temperature programming was from 50 to 230ºC. Individual FAMEs were identified by reference to authentic standards and, when necessary, further confirmation of identity of the FAs was carried out by GC-MS (DSQ II, Thermo Scientific). Prior to transmethylation, nonadecanoic acid (19:0) was added to the lipid fractions as an internal standard. The results were expressed as µg fatty

acid/mg cell protein or mg fatty acid/100g wet weight of muscle for total fatty acid contents and as weight percentage of TL for individual fatty acids.

2.9. Statistical analysis

Results are presented as mean ± SD, except those of tissue expression where log 10 mean normalised ratios ± SE was used. Principal components analysis (PCA) was performed to assess FA composition of non-radioactive enterocytes and hepatocytes, as well as muscle and diet. Data were checked for normal distribution with the one-sample Shapiro-Wilk test, as well as for homogeneity of the variances with the Levene's test (Zar, 1999). One-way ANOVA test followed by a Tukey HSD multiple comparison test was performed for tissue incorporation and transformation of radioactivity as well as for tissue expression of each enzyme. When normal distribution and/or homoscedasticity was not achieved, data were arcsine transformed and when necessary data were subjected to the Kruskall-Wallis non-parametric test, followed by Dunnett T3 (Zar, 1999). Statistical significance was established at $P < 0.05$. Statistical analyses were performed using the SPSS for Windows 21 statistical package (SPSS Inc., New York, USA).

3. Results and Discussion

3.1 Sequences and phylogenetic analysis of fads2, elovl5 and elovl2

Fads2 desaturase and Elovl2 and Elovl5 elongases of tench were constituted by an ORF of 1335, 885 and 876 bp, respectively, encoding putative proteins of 444, 294 and 291 aa, respectively, which were deposited in the GenBank database under the accession numbers: MN702459, MN702460 and MN702461, respectively. The phylogenetic tree for Fads2 of tench showed a closer clustering with Fads2 from cyprinids carp and zebrafish (*Cyprinus carpio* and *D. rerio*), African catfish (*C. gariepinus*) and tambaqui (*Colossoma macropomum*) and they were clustered within the Fads2 branch (Fig. 2). Both Elovl2 and Elovl5 from tench were closely grouped with corresponding orthologues from zebrafish, African catfish and tambaqui (Fig. 3). Therefore, phylogenetic clustering could confirm the expected putative functionality of the enzymes studied in the present report.

3.2. Functional characterization

The tench Fads2 showed Δ6 and Δ5 activities. Thus, through a Δ6 activity, 18:2n-6 and 18:3n-3 were converted to 18:3n-6 and 18:4n-3, respectively, while 20:4n-6 and 20:5n-3 were obtained by Δ5 activity from 20:3n-6 and 20:4n-3, respectively (Table 3). Similar dual Δ6Δ5 desaturases Fads2 have been previously found in other species such as *C. striata*, *C. estor*, *C. gariepinus*, *C. carpio*, *D. rerio*, cobia *R. canadum*, and *S. canaliculatus* (Fonseca-Madrigal et al., 2014; Hastings et al., 2001; Kuah et al., 2016; Li et al., 2010; Oboh et al., 2016; Zheng et al., 2004, 2009). Non-bifunctional Fads2 activities have also been reported in different species, being Δ6 activity the most common activity in marine and freshwater fish (Castro et al., 2016). For instance, in *E. coioides*, *Paralichthys olivaceus* and *Scatophagus argus* only Fads2 Δ6 activity has

been reported (Kabeya et al., 2017; Li et al., 2014; Xie et al., 2014) whereas Δ5 and Δ4 but not Δ6 activity has been described for *C. striata*, *C. estor* and *S. canaliculatus* (Fonseca-Madrigal et al., 2014; Kuah et al., 2016; Li et al., 2010). Therefore, fish show a high variability in their Fads2 desaturase activities, being able to act over a wider range of substrates than mammalian species, which mainly show Δ6 function (Castro et al., 2016). The environment (marine or freshwater) and trophic level have been speculated as plausible causes for the high diversity over substrates of Fads2 in fish (Morais et al., 2012). However, this hypothesis has not yet been proved, and as suggested by Garrido et al. (2019), phylogenetic background might have a higher influence.

The newly cloned tench fatty acyl elongases showed activity towards most of PUFA substrates assayed (Table 4). This is largely in agreement with functions of Elovl5 from *Argyrosomus regius*, *C. striata*, *D. rerio*, and *S. senegalensis*, which preferentially elongated C_{18} and C_{20} PUFA substrates (Agaba et al., 2005; Kuah et al., 2015; Monroig et al., 2013; Morais et al., 2012). Moreover, and consistently with the functions of the *D. rerio* and *S. salar* Elovl2 (Monroig et al., 2009; Morais et al., 2009), the tench Elovl2 showed higher conversions towards C_{20} and C_{22} than over C_{18} substrates (Table 4). Nevertheless, Gregory and James (2014) did not find activity of Elovl2 towards C_{18} substrates in *O. mykiss*, while Oboh et al. (2016) reported higher conversion for some C_{18} substrates than for ω6 C_{22} in *C. gariepinus*. All above suggests that Elovl2 affinity and preferential conversion over substrates of different length is species specific (Castro et al., 2016).

3.3. Tissue expression of *fads2, elovl5* and *elovl2* in tench

In our study, liver displayed the highest expression levels of *fads2, elovl2* and *elovl5*

414 followed by those of gut and/or brain (Fig. 4). The highest expression in liver would
415 demonstrate the importance of this tissue for the overall production of LC-PUFA in
416 tench. A similar pattern was observed in zebrafish (Monroig et al., 2009) while in
417 Atlantic salmon, tissue distribution was gut > liver ≥ brain (Morais et al., 2009). By
418 contrast, other freshwater species such as striped snakehead (*C. striata*) and silver barb
419 (*B. gonionotus*) presented the highest expression of *fads2* and *elovl5* in brain
420 (Janaranjani et al., 2018; Kuah et al., 2016). In our present work, the lowest expression
421 for *fads2* and *elovl5* was detected in tench muscle whereas heart were the tissues with
422 the lowest expression of *elovl2*, followed by gill, spleen and muscle. Similarly, the
423 lowest expression of *elovl2* in *S. salar* and *D. rerio* was found in white muscle and gill,
424 respectively (Monroig et al., 2009; Morais et al., 2009).
425
426 **3.4 Fatty acid composition of enterocytes, hepatocytes and muscle**
427 In all cell types/tissue studied in the present work, 18:1n-9 followed by 16:0, 22:6n-3
428 and 18:2n-6 were the most abundant FAs (Table 5). These FAs were also predominant
429 in tench fed an experimental diet supplemented with rapeseed oil or when fish meal was
430 substituted by poultry by-product meal (Ljubojević et al., 2014; Panicz et al., 2017) and
431 also in wild specimens (Vasconi et al., 2015). A principal component analysis (PCA)
432 was used to examine the possible effect of the diet into target cells/tissue (Fig. 5). The
433 first two components (PC1 and PC2) in the PCA explained 77.0% of variation. PC1
434 explained 49.5% of variation, with 18:1n-9, 20:4n-6, 22:6n-3, 18:3n-3, 18:0 and 18:2n-6
435 showing the highest contribution (Fig. 5A). PC1 clearly separated AA, DHA and 18:0
436 from 18:1n-9, 18:3n-3 and 18:2n-6. PC2 displayed a lower contribution with 27.5% of
437 the variation explained and with the highest weight for 14:0 and 18:1n-7. The plot
438 distribution of individual factor scores of replicated tissues and diet is shown in Figure

5B. In factor score 1, muscle and diet clustered together but separated from enterocytes, while hepatocytes showed an intermediate composition between them. It is well known that dietary FA may affect fish muscle FA composition (Pérez et al., 2014), which is in agreement with our present PCA-results particularly for 18:1n-9, 18:2n-6 and 18:3n-3 which proportions in muscle remained fairly constant with respect to dietary levels despite their variations in cells. In this sense, it is noteworthy to mention the 6-fold increase of AA and the 3-fold increase of DHA in enterocytes compared to diet, indicating their active role in up-taking these LC-PUFA from lipid digestion (Oxley et al., 2005; Pérez et al., 1999) and, therefore, in increasing their bioavailability. Enterocytes have also shown a more relevant function in the biosynthesis of LC-PUFA than hepatocytes in species as cod (Tocher et al., 2006). Important (and abundant) lipid molecules tightly associated to membrane physical properties in living epithelial cells are phospholipids rich in polyunsaturated fatty acids including DHA, which play an important role in a number of physiological processes and adaptive responses suggesting a close relationship between the composition of cell membranes and the osmo- and ionoregulate functions of these epithelials (Díaz et al., 2016; Sargent et al., 1995). In contrast to 18:3n-3, which is always present in lower percentages in the isolated cells and in fish flesh compared to the diet supply, DHA is magnified in all tissues analysed (see Tables 1 and 5). The above mentioned LC-PUFA biosynthetic capacity expressed in tench tissues could explain in part these surprisingly high levels of DHA found in flesh from this freshwater species. In factor score 2, 18:1n-7 seemed to have a higher contribution to the differences among hepatocytes and the remaining clusters which were associated to 14:0 content. The saturated FA could be absorbed by enterocytes from the diet, re-esterified and transported by the blood until finally deposited in the muscle (Henderson, 1996) whereas the higher content of 18:1n-7 in the

hepatocytes could suggest its possible biosynthesis in this tissue.

3.5. Fatty acid metabolism in isolated enterocytes and hepatocytes

All radioactive substrates were similarly incorporated into tench enterocytes (49-61 pmol/mg prot · h; Table 6a). The incorporation of radioactivity into tench hepatocytes lipids neither significantly vary among fatty acids (62-75 pmol/mg prot · h; Table 6a).

Both enterocytes and hepatocytes also showed similar trends in their transformation capacity of radiolabelled fatty acids (Table 6a). Thus, 20:5n-3 was the most modified substrate (24-25%) in both cell types being mainly elongated to 22:5n-3 but also further elongated up to C_{28} FA (Table 6b). Heterologous expression of the *D. rerio* Elovl2 in yeast evidenced the elongation of 20:5n-3 up to 26:5n-3 (Monroig et al., 2009). Indeed, Elovl2 has been reported to be involved in the biosynthesis of FA up to C_{30} in mice (Zadravec et al., 2011), although the action of Elovl4 cannot be ruled out since this enzyme has been demonstrated to be involved in the biosynthesis of polyenes up to C_{36} in zebrafish (Monroig et al., 2010a). Therefore, the elongation products found in our study could be produced by these enzymes. Moreover, Mourente and Tocher (1994) reported that gilthead seabream (*S. aurata*) has the capacity to elongate 20:5n-3 to 24:5n-3, which can be subsequently desaturated and chain shortened to produce 22:6n-3 (Oboh et al., 2017; Sprecher, 2000). In our study, no DHA was obtained from the incubation with EPA, which could be due to an inhibitory effect of EPA into LC-PUFA synthesis. In fact, the addition of EPA in incubated cells with radiolabelled 18:3n-3 has shown to decrease the Δ6 activity toward C_{24} (Kjaer et al., 2016).

Tench enterocytes presented similar rates of elongation and desaturation over both 18:2n-6 and 18:3n-3. However, *de novo* fatty acid synthesis was only observed upon incubation with 18:2n-6 (Table 6a). This *de novo* synthesis is evidenced by the presence

of radiolabelled bands in the TLC plates corresponding to shorter FAs produced by using the [1-^{14}C] released after a first β-oxidation cycle of the labelled substrate. Therefore, and although the β-oxidation rate was not directly measured in our assay (for further details see Díaz-López et al., 2010), the present results suggest that at least under the above described culture conditions and dietary regime, 18:2n-6 is more efficiently used for β-oxidation by tench in comparison to 18:3n-3. Activation of *de novo* synthesis of saturated and monounsaturated FA has been reported in cyprinid as a result of an unbalanced intake of 18:2n-6 (Farkas et al., 1978). Despite both LA and ALA are widely considered good substrates for β-oxidation in fish, and thus, good energy sources (Brown, 2016; Chen et al., 2018), our results could also suggest that the dietary 18:2n-6/18:3n-3 ratio might be unbalanced for this species. Nonetheless, other hypothesis cannot completely be ruled out.

On the contrary, in hepatocytes, elongation and elongation/desaturation activities over 18:2n-6 were higher than those over 18:3n-3 while the opposite trend was observed for desaturation (Table 6a). Higher Δ6 desaturation products from 18:3n-3 in hepatocytes of *S. salar* have been associated to receiving a diet rich in n6 FA (Bou et al., 2017) indicating that the diet given to our experimental tench probably fails to supply a right balance of n3/n6 FA for this species.

Interestingly, no direct elongation of 18:3n-3 towards 20:3n-3 was detected in hepatocytes (Table 6b). The absence of the labelled intermediary 20:3n-3 in our study could be related to a reduced bioavailability of EPA and/or DHA, since in Atlantic salmon an increment of 20:3n-3 from labelled 18:3n-3 was observed associated to a higher dietary level of EPA and/or DHA (Bou et al., 2017).

24:5n-6 was detected in enterocytes and hepatocytes when incubated with [1-^{14}C] 18:2n-6, whereas 24:6n-3 was only found from [1-^{14}C] 18:3n-3 in enterocytes. This

514 suggests that the possible route of DHA biosynthesis from EPA consists of two
515 consecutive elongation steps to 24:5n-3, which is then converted by a Δ6 desaturase into
516 24:6n-3 before the latter is chain-shortened to DHA. This capacity to synthesise DHA
517 from C_{18} precursors has been reported in other freshwater species such as carp, tilapia
518 and trout and anadromous Atlantic salmon (Buzzi et al., 1996; Olsen et al., 1990;
519 Ruyter et al., 2003; Tocher and Dick, 1999). The fact that DHA was detected after
520 incubation with [1-^{14}C] 18:3n-3 but not from [1-^{14}C] EPA, could be associated to an
521 inhibitory effect of EPA into LC-PUFA synthesis as previously discussed (Kjaer et al.,
522 2016).
523
524 **4. Conclusions**
525 In the present study a Fads2 with a bifunctional activity Δ6/Δ5, and two elongases
526 (Elovl2 and Elovl5) have been molecularly and functionally characterized from tench.
527 These activities were further confirmed by studies developed in fresh isolated
528 enterocytes and hepatocytes. Products derived from Δ6 activity over C_{24} as well as
529 products from β-oxidation and/or other enzymes involved in FA elongation/desaturation
530 such as 22:5n-6 or 22:6n-3 for n-6 and n-3 series, respectively, were also detected. All
531 above confirms the ability of tench to produce DHA from 18:3n-3. However, *de novo*
532 synthesis of some fatty acids over [1-^{14}C] released from 18:2n-6 substrate β-oxidation,
533 the high desaturation activity over 18:3n-3 in isolated enterocytes and hepatocytes, as
534 well as the lack of detection of labelled 20:3n-3 in hepatocytes could suggest that the
535 diet used in this study did not supply a balanced 18:2n-6/18:3n-3 ratio for this species.
536 In view of the present results it is hypothesised that providing a better balanced dietary
537 supply of 18:2n-6/18:3n-3 (diminishing 18:2n-6 and rising 18:3n-3 content) the DHA
538 flesh content could be increased improving the nutritional value of tench as well as its

potential for aquaculture diversification and sustainability.

Acknowledgements

This study was funded by Ministerio de Economía y Competitividad (AGL2015-70994-R). Authors thank the collaboration of the Centro Regional de Acuicultura "Las Vegas del Guadiana" (Villafranco del Guadiana, Spain). A. Galindo and M. Marrero are financed by a PhD grant by Cajasiete and Gobierno de Canarias, respectively. Dr. Covadonga Rodríguez is a member of the Instituto de Tecnologías Biomédicas de Canarias (ITB). We also thank Dr. Inmaculada Giráldez from Universidad de Huelva for her assistance with laboratory facilities and Dr. Deiene Rodríguez Barreto for her useful revision and assistance with clarification of the manuscript.

549 **References**

550 Agaba, M.K., Tocher, D.R., Zheng, X., Dickson, C.A., Dick, J.R., Teale, A.J., 2005.
551 Cloning and functional characterisation of polyunsaturated fatty acid elongases of
552 marine and freshwater teleost fish. Comp. Biochem. Physiol. Part B Biochem. Mol.
553 Biol. 142, 342–352.

554 Béné, C., Barange, M., Subasinghe, R., Pinstrup-Andersen, P., Merino, G., Hemre, G.-
555 I., Williams, M., 2015. Feeding 9 billion by 2050 - Putting fish back on the menu.
556 Food Secur. 7, 261–274.

557 Bou, M., Østbye, T.-K., Berge, G.M., Ruyter, B., 2017. EPA, DHA, and lipoic acid
558 differentially modulate the n-3 fatty acid biosynthetic pathway in Atlantic salmon
559 hepatocytes. Lipids 52, 265–283.

560 Brown, R.A., 2016. The crucial relevance of ALA and LA as primary peroxisomal beta-
561 oxidation substrates, of oxidised LA as the primary endogenous activator of PPAR
562 gamma, and energy deficit as the primary activator of PPAR alpha, in: Hegde,
563 M.V., Zanwar, A.A., and Adeka, S.P. (Eds.), Omega-3 Fatty Acids. Springer,
564 Cham, pp. 451-463.

565 Buzzi, M., Henderson, R.J., Sargent, J.R., 1996. The desaturation and elongation of
566 linolenic acid and eicosapentaenoic acid by hepatocytes and liver microsomes from
567 rainbow trout (*Oncorhynchus mykiss*) fed diets containing fish oil or olive oil.
568 Biochim. Biophys. Acta 1299, 235–244.

569 Capella-Gutiérrez, S., Silla-Martínez, J.M., Gabaldón, T., 2009. TrimAl: a tool for
570 automated alignment trimming in large-scale phylogenetic analyses.
571 Bioinformatics 25(15), 1972-1973.

572 Castro, L.F.C., Tocher, D.R., Monroig, O., 2016. Long-chain polyunsaturated fatty acid
573 biosynthesis in chordates: Insights into the evolution of Fads and Elovl gene

574 repertoire. Prog. Lipid Res. 62, 25–40.
575 Celada, J.D., Aguilera, A., García, V., Carral, J.M., Sáez-Royuela, M., González, R.,
576 González, Á., 2009. Rearing juvenile tench (*Tinca tinca* L.) under controlled
577 conditions using Artemia nauplii as supplement to a dry diet. Aquac. Int. 17, 565-
578 570.
579 Chen, C., Guan, W., Xie, Q., Chen, G., He, X., Zhang, H., Guo, W., Chen, Y., Pan, Q,
580 2018. n-3 essential fatty acids in Nile tilapia, *Oreochromis niloticus*: Bioconverting
581 LNA to DHA is relatively efficient and the LC-PUFA biosynthetic pathway is
582 substrate limited in juvenile fish. Aquaculture 495, 513-522.
583 Christie, W.W., Han, X., 2010. Lipid analysis : Isolation, separation, identification and
584 lipidomic analysis. Oily Press, an imprint of PJ Barnes & Associates.
585 Darriba, D., Posada, D., Kozlov, A.M., Stamatakis, A., Morel, B., Flouri, T., 2019.
586 ModelTest-NG: a new and scalable tool for the selection of DNA and protein
587 evolutionary models. BioRxiv, 612903.
588 de Roos, B., Sneddon, A.A., Sprague, M., Horgan, G.W., Brouwer, I.A., 2017. The
589 potential impact of compositional changes in farmed fish on its health-giving
590 properties: is it time to reconsider current dietary recommendations? Public Health
591 Nutr. 20, 2042–2049.
592 Díaz, M., Dópido, R., Gómez, T., Rodríguez, C., 2016. Membrane lipid
593 microenvironment modulates thermodynamic properties of the Na+-K+-ATPase in
594 branchial and intestinal epithelia in euryhaline fish in vivo. Front. Physiol. 7, 589.
595 FAO Fisheries and Aquaculture Department, 2017. Fisheries and aquaculture software.
596 FishStatJ - software for fishery statistical time series.
597 Farkas, T., Csengeri, I., Majoros, F., Oláh, J., 1978. Metabolism of fatty acids in fish. II.
598 Biosynthesis of fatty acids in relation to diet in the carp, *Cyprinus carpio* Linnaeus

1758. Aquaculture 14, 57–65.

Fonseca-Madrigal, J., Navarro, J.C., Hontoria, F., Tocher, D.R., Martínez-Palacios, C.A., Monroig, Ó., 2014. Diversification of substrate specificities in teleostei Fads2: characterization of Δ4 and Δ6Δ5 desaturases of *Chirostoma estor*. J. Lipid Res. 55, 1408–1419.

García, V., Celada, J.D., González, R., Carral, J.M., Sáez-Royuela, M., González, Á., 2015. Response of juvenile tench (*Tinca tinca* L.) fed practical diets with different protein contents and substitution levels of fish meal by soybean meal. Aquac. Res. 46, 28–38.

Garrido, D., Kabeya, N., Betancor, M.B., Pérez, J.A., Acosta, N.G., Tocher, D.R., Rodríguez, C., Monroig, O., 2019. Functional diversification of teleost Fads2 fatty acyl desaturases occurs independently of the trophic level. Sci. Rep. 9:11199.

González-Rodríguez, Á., Celada, J.D., Carral, J.M., Sáez-Royuela, M., Fuertes, J.B., 2014. Evaluation of a practical diet for juvenile tench (*Tinca tinca* L.) and substitution possibilities of fish meal by feather meal. Anim. Feed Sci. Technol. 187, 61–67.

Gregory, M.K., James, M.J., 2014. Rainbow trout (*Oncorhynchus mykiss*) Elovl5 and Elovl2 differ in selectivity for elongation of omega-3 docosapentaenoic acid. Biochim. Biophys. Acta 1841, 1656–1660.

Hastings, N., Agaba, M., Tocher, D.R., Leaver, M.J., Dick, J.R., Sargent, J.R., Teale, A.J., 2001. A vertebrate fatty acid desaturase with Delta 5 and Delta 6 activities. Proc. Natl. Acad. Sci. U. S. A. 98, 14304–9.

Henderson, R.J., 1996. Fatty acid metabolism in freshwater fish with particular reference to polyunsaturated fatty acids. Arch. für Tierernaehrung 49, 5–22.

Jakobsson, A., Westerberg, R., Jacobsson, A., 2006. Fatty acid elongases in mammals:

624 Their regulation and roles in metabolism. Prog. Lipid Res. 45, 237–249.
625 Janaranjani, M., Mah, M.-Q., Kuah, M.-K., Fadhilah, N., Hing, S.-R., Han, W.-Y., Shu-
626 Chien, A.C., 2018. Capacity for eicosapentaenoic acid and arachidonic acid
627 biosynthesis in silver barb (*Barbonymus gonionotus*): Functional characterisation
628 of a Δ6/Δ8/Δ5 Fads2 desaturase and Elovl5 elongase. Aquaculture 497, 469–486.
629 Kabeya, N., Chiba, M., Haga, Y., Satoh, S., Yoshizaki, G., 2017. Cloning and
630 functional characterization of fads2 desaturase and elovl5 elongase from Japanese
631 flounder *Paralichthys olivaceus*. Comp. Biochem. Physiol. 214, 36–46.
632 Katoh, K., Rozewicki, J., Yamada, K.D., 2017. MAFFT online service: multiple
633 sequence alignment, interactive sequence choice and visualization. Brief.
634 Bioinform. bbx108-bbx108.
635 Kjær, M.A., Ruyter, B., Berge, G.M., Sun, Y., Østbye, T.K.K. 2016. Regulation of the
636 omega-3 fatty acid biosynthetic pathway in Atlantic salmon hepatocytes. PloS one,
637 11(12), e0168230.
638 Kuah, M.-K., Jaya-Ram, A., Shu-Chien, A.C., 2015. The capacity for long-chain
639 polyunsaturated fatty acid synthesis in a carnivorous vertebrate: Functional
640 characterisation and nutritional regulation of a Fads2 fatty acyl desaturase with Δ4
641 activity and an Elovl5 elongase in striped snakehead (*Channa striata*). Biochim.
642 Biophys. Acta 1851, 248–260.
643 Kuah, M.-K., Jaya-Ram, A., Shu-Chien, A.C., 2016. A fatty acyl desaturase (fads2)
644 with dual Δ6 and Δ5 activities from the freshwater carnivorous striped snakehead
645 *Channa striata*. Comp. Biochem. Physiol. Part A 201, 146–155.
646 Letunic, I., Bork, P., 2016. Interactive tree of life (iTOL) v3: an online tool for the
647 display and annotation of phylogenetic and other trees. Nucleic Acids Res. 44,
648 W242–W245.

649 Li, S., Mai, K., Xu, W., Yuan, Y., Zhang, Y., Ai, Q., 2014. Characterization, mRNA
650 expression and regulation of Δ6 fatty acyl desaturase (FADS2) by dietary n − 3
651 long chain polyunsaturated fatty acid (LC-PUFA) levels in grouper larvae
652 (*Epinephelus coioides*). Aquaculture 434, 212–219.
653 Li, Y., Monroig, O., Zhang, L., Wang, S., Zheng, X., Dick, J.R., You, C., Tocher, D.R.,
654 2010. Vertebrate fatty acyl desaturase with Δ4 activity. Proc. Natl. Acad. Sci. U. S.
655 A. 107, 16840–16845.
656 Ljubojević, D., Ćirković, M., Novakov, N., Puvača, N., Aleksić, N., Lujić, J.,
657 Jovanović, R., 2014. Comparison of meat quality of tench, *Tinca tinca,* reared in
658 extensive and semi-intensive culture systems. J. Appl. Ichthyol. 30, 50–57.
659 Lopes-Marques, M., Ozório, R., Amaral, R., Tocher, D.R., Monroig, Ó., Castro, L.F.C.
660 2017. Molecular and functional characterization of a *fads2* orthologue in the
661 Amazonian teleost, *Arapaima gigas*. Comp. Biochem. Physiol. 203, 84-91.
662 Lowry, O.H., Rosebrough, N.J., Farr, A.L., Randall, R.L., 1951. Protein asurement with
663 the folin phenol reagent. J. Biol. Chem. 193(1), 265–275.
664 Monroig, Ó., Rotllant, J., Sánchez, E., Cerdá-Reverter, J.M., Tocher, D.R., 2009.
665 Expression of long-chain polyunsaturated fatty acid (LC-PUFA) biosynthesis
666 genes during zebrafish *Danio rerio* early embryogenesis. Biochim. Biophys. Acta -
667 Mol. Cell Biol. Lipids 1791, 1093–1101.
668 Monroig, Ó., Rotllant, J., Cerdá-Reverter, J.M., Dick, J.R., Figueras, A., Tocher, D.R.,
669 2010a. Expression and role of Elovl4 elongases in biosynthesis of very long-chain
670 fatty acids during zebrafish *Danio rerio* early embryonic development. Biochim.
671 Biophys. Acta - Mol. Cell Biol. Lipids 1801, 1145–1154.
672 Monroig, Ó., Zheng, X., Morais, S., Leaver, M.J., Taggart, J.B., Tocher, D.R., 2010b.
673 Multiple genes for functional 6 fatty acyl desaturases (Fad) in Atlantic salmon

(*Salmo salar* L.): Gene and cDNA characterization, functional expression, tissue distribution and nutritional regulation. Biochim. Biophys. Acta 1801, 1072–1081.

Monroig, Ó., Li, Y., Tocher, D.R., 2011. Delta-8 desaturation activity varies among fatty acyl desaturases of teleost fish: High activity in delta-6 desaturases of marine species. Comp. Biochem. Physiol. 159, 206–213.

Monroig, Ó., Tocher, D.R., Hontoria, F., Navarro, J.C., 2013. Functional characterisation of a Fads2 fatty acyl desaturase with Δ6/Δ8 activity and an Elovl5 with C16, C18 and C20 elongase activity in the anadromous teleost meagre (*Argyrosomus regius*). Aquaculture 412–413, 14–22.

Monroig, O., Tocher, D.R., Castro, L.F.C., 2018. Polyunsaturated fatty acid biosynthesis and metabolism in fish, in: Burdge, G.. (Ed.), Polyunsaturated Fatty Acid Metabolism. AOCS Press, London, pp. 31–60.

Morais, S., Monroig, O., Zheng, X., Leaver, M.J., Tocher, D.R., 2009. Highly unsaturated fatty acid synthesis in Atlantic salmon: Characterization of ELOVL5- and ELOVL2-like elongases. Mar. Biotechnol. 11, 627–639.

Morais, S., Castanheira, F., Martinez-Rubio, L., Conceição, L.E.C., Tocher, D.R., 2012. Long chain polyunsaturated fatty acid synthesis in a marine vertebrate: Ontogenetic and nutritional regulation of a fatty acyl desaturase with Δ4 activity. Biochim. Biophys. Acta 1821, 660–671.

Mourente, G., Tocher, D.R., 1994. In vivo metabolism of [1-14C]linolenic acid (18:3(n − 3)) and [1-14C]eicosapentaenoic acid (20:5(n − 3)) in a marine fish: Time-course of the desaturation/elongation pathway. Biochim. Biophys. Acta 1212, 109–118.

Oboh, A., Betancor, M.B., Tocher, D.R., Monroig, O., 2016. Biosynthesis of long-chain polyunsaturated fatty acids in the African catfish *Clarias gariepinus*: Molecular cloning and functional characterisation of fatty acyl desaturase (fads2) and

699 elongase (elovl2) cDNAs7. Aquaculture 462, 70–79.
700 Oboh, A., Kabeya, N., Carmona-Antoñanzas, G., Castro, L.F.C., Dick, J.R., Tocher,
701 D.R., Monroig, O., 2017. Two alternative pathways for docosahexaenoic acid
702 (DHA, 22:6n-3) biosynthesis are widespread among teleost fish. Sci. Rep. 7, 3889.
703 Olsen, R.E., Henderson, R.J., McAndrew, B.J., 1990. The conversion of linoleic acid
704 and linolenic acid to longer chain polyunsaturated fatty acids by Tilapia
705 (*Oreochromis nilotica*) in vivo. Fish Physiol. Biochem. 8, 261–270.
706 Oxley, A., Tocher, D.R., Torstensen, B.E., Olsen, R.E., 2005. Fatty acid utilisation and
707 metabolism in caecal enterocytes of rainbow trout (*Oncorhynchus mykiss*) fed
708 dietary fish or copepod oil. Biochim. Biophys. Acta 1737, 119–129.
709 Panicz, R., 2016. Validation of reference genes for RT-qPCR analysis of growth
710 hormone receptor and growth hormone expression in the tench (*Tinca tinca*) fed
711 substituting poultry meal for fish meal. Aquaculture 465, 179–188.
712 Panicz, R., Żochowska-Kujawska, J., Sadowski, J., Sobczak, M., 2017. Effect of
713 feeding various levels of poultry by-product meal on the blood parameters, filet
714 composition and structure of female tenches (*Tinca tinca*). Aquac. Res. 48, 5373–
715 5384.
716 Pérez, J.A., Rodríguez, C., Henderson, R.J., 1999. The uptake and esterification of
717 radiolabelled fatty acids by enterocytes isolated from rainbow trout (*Oncorhynchus*
718 *mykiss*). Fish Physiol. Biochem. 20, 125–134.
719 Pérez, J.A., Rodríguez, C., Bolaños, A., Cejas, J.R., Lorenzo, A., 2014. Beef tallow as
720 an alternative to fish oil in diets for gilthead sea bream (*Sparus aurata*) juveniles:
721 Effects on fish performance, tissue fatty acid composition, health and flesh
722 nutritional value. Eur. J. Lipid Sci. Tech. 116(5), 571-583.
723 Pula, H.J., Trenzado, C.E., García-Mesa, S., Fallola, C., Sanz, A., 2018. Effects of

different culture systems on growth, immune status, and other physiological parameters of tench (*Tinca tinca*). Aquaculture 485, 101–110.

Ren, H., Yu, J., Xu, P., Tang, Y., 2012. Influence of dietary fatty acids on muscle fatty acid composition and expression levels of Δ6 desaturase-like and Elovl5-like elongase in common carp (*Cyprinus carpio* var. Jian). Comp. Biochem. Physiol. Part B 163, 184–192.

Rodríguez, C., Pérez, J.A., Henderson, R.J., 2002. The esterification and modification of n-3 and n-6 polyunsaturated fatty acids by hepatocytes and liver microsomes of turbot (*Scophthalmus maximus*). Comp. Biochem. Physiol. Part B 132, 559–570.

Rodríguez, R., Celada, J.D., Sáez-Royuela, M., Carral, J.M., Aguilera, A., Melendre, P.M., 2004. Artificial reproduction in 1-year-old tench (*Tinca tinca* L.). J. Appl. Ichthyol. 20, 542–544.

Ruyter, B., Røjø, C., Grisdale-Helland, B., Rosenlund, G., Obach, A., Thomassen, M.S., 2003. Influence of temperature and high dietary linoleic acid content on esterification, elongation, and desaturation of PUFA in Atlantic salmon hepatocytes. Lipids 38, 833–840.

Sargent, J.R., 1995. Origins and functions of (n-3) polyunsaturated fatty acids in marine organisms. In Proceedings, International Phospholipid Conference (Hamburg). (pp. 250-261). American Oil Chemists Society Press.

Sprecher, H., 2000. Metabolism of highly unsaturated n-3 and n-6 fatty acids. Biochim. Biophys. Acta 1486, 219–231.

Tanomman, S., Ketudat-Cairns, M., Jangprai, A., Boonanuntanasarn, S., 2013. Characterization of fatty acid delta-6 desaturase gene in Nile tilapia and heterogenous expression in *Saccharomyces cerevisiae*. Comp. Biochem. Physiol. Part B 166, 148–156.

749 Tocher, D.R., 2015. Omega-3 long-chain polyunsaturated fatty acids and aquaculture in
750 perspective. Aquaculture 449, 94–107.
751 Tocher, D.R., Dick, J.R., 1999. Polyunsaturated fatty acid metabolism in a cell culture
752 model of essential fatty acid deficiency in a freshwater fish, carp (*Cyprinus*
753 *carpio*). Fish Physiol. Biochem. 21, 257–267.
754 Tocher, D.R., Agaba, M., Hastings, N., Teale, A.J., 2003. Biochemical and molecular
755 studies of the fatty acid desaturation pathway in fish. In: Browman, H.I.,
756 Skiftesvik, A.B. (Eds.), The Big Fish Bang: Proceedings of the 26th Annual Larval
757 Fish Conference. Institute of Marine Nutrition, Bergen, Norway, pp. 211–227.
758 Tocher, D.R., Zheng, X., Schlechtriem, C., Hastings, N., Dick, J.R., Teale, A.J., 2006.
759 Highly unsaturated fatty acid synthesis in marine fish: Cloning, functional
760 characterization, and nutritional regulation of fatty acyl Δ6 desaturase of Atlantic
761 cod (*Gadus morhua* L.). Lipids 41, 1003–1016.
762 Vandesompele, J., De Preter, K., Pattyn, F., Poppe, B., Van Roy, N., De Paepe, A.,
763 Speleman, F., 2002. Accurate normalization of real-time quantitative RT-PCR data
764 by geometric averaging of multiple internal control genes. Genome Biol. 3(7),
765 research 0034.
766 Vasconi, M., Caprino, F., Bellagamba, F., Busetto, M.L., Bernardi, C., Puzzi, C.,
767 Moretti, V. M., 2015. Fatty acid composition of freshwater wild fish in subalpine
768 lakes: a comparative study. Lipids, 50(3), 283-302.
769 Vinatea, L., Malpartida, J., Carbó, R., Andree, K.B., Gisbert, E., Estévez, A., 2018. A
770 comparison of recirculation aquaculture systems versus biofloc technology culture
771 system for on-growing of fry of *Tinca tinca* (Cyprinidae) and fry of grey *Mugil*
772 *cephalus* (Mugilidae). Aquaculture 482, 155–161.
773 Wang, J., Min, W., Guan, M., Gong, L., Ren, J., Huang, Z., Zheng, H., Zhang, J., Liu,

774 H., Han, Y., 2006. Tench farming in China: present status and future prospects.
775 Aquac. Int. 14, 205–208.
776 Wolnicki, J., Myszkowski, L., Korwin-kossakowski, M., Kamiński, R., Stanny, L.A.,
777 2006. Effects of different diets on juvenile tench, *Tinca tinca* (L.) reared under
778 controlled conditions. Aquac. Int. 14, 89–98.
779 Xie, D., Chen, F., Lin, S., Wang, S., You, C., Monroig, Ó., Tocher, D.R., Li, Y., 2014.
780 Cloning, functional characterization and nutritional regulation of Δ6 fatty acyl
781 desaturase in the herbivorous euryhaline teleost *Scatophagus Argus*. PLoS One 9,
782 e90200.
783 Zadravec, D., Tvrdik, P., Guillou, H., Haslam, R., Kobayashi, T., Napier, J. A.,
784 Capecchi, M.R., Jacobsson, A., 2011. ELOVL2 controls the level of n-6 28:5 and
785 30:5 fatty acids in testis, a prerequisite for male fertility and sperm maturation in
786 mice. J. Lipid Res. 52(2), 245-255.
787 Zar, J.H., 1999. Biostatistical Analysis, 4th ed. Prentice-Hall Inc., Upper Saddle River.
788 Zheng, X., Ding, Z., Xu, Y., Monroig, O., Morais, S., Tocher, D.R., 2009. Physiological
789 roles of fatty acyl desaturases and elongases in marine fish: Characterisation of
790 cDNAs of fatty acyl Δ6 desaturase and elovl5 elongase of cobia (*Rachycentron*
791 *canadum*). Aquaculture 290, 122–131.
792 Zheng, X., Seiliez, I., Hastings, N., Tocher, D.R., Panserat, S., Dickson, C.A., Bergot,
793 P., Teale, A.J., 2004. Characterization and comparison of fatty acyl Δ6 desaturase
794 cDNAs from freshwater and marine teleost fish species. Comp. Biochem. Physiol.
795 Part B 139, 269–279.
796

797 **Table 1.** Total lipid (% dry weight), total FA (mg
798 fatty acid/g dry weight) and main fatty acid
799 composition (% of total FA) of *Tinca tinca* diet.

	Diet
Total lipid	19.0 ± 0.2
Total FA	146.9 ± 2.9
Fatty acid	
14:0	1.9 ± 0.0
16:0	17.2 ± 0.0
18:0	5.6 ± 0.1
Total saturates[1]	26.0 ± 0.0
16:1n-7	3.8 ± 0.0
18:1n-9	36.5 ± 0.1
18:1n-7	3.2 ± 0.1
20:1n-9	1.5 ± 0.0
Total monoenes[1]	46.8 ± 0.1
18:2n-6	13.1 ± 0.0
18:3n-6	nd
20:3n-6	nd
20:4n-6	0.6 ± 0.0
22:5n-6	0.3 ± 0.0
Total n-6 PUFA[1]	14.3 ± 0.0
18:3n-3	2.7 ± 0.0
20:5n-3	2.7 ± 0.1
22:5n-3	0.5 ± 0.0
22:6n-3	4.4 ± 0.0
Total n-3 PUFA[1]	11.1 ± 0.2
n-3/n-6	0.8 ± 0.0
Total n-3 LC-PUFA	7.8 ± 0.1

800 Results are presented as mean ± SD (n=2). nd; no
801 detected. [1] Includes other minor components not
802 shown.

Table 2. Sequences of the primer pairs used in the cloning of the tench fatty acyl desaturase (Fads2) and elongases (Elovl2 and Elovl5), ORF and RT-PCR analysis of gene expression in tench tissues. Restriction sites are underlined; *Bam*H I were in forward primers except to Elovl5 where it was *Hin*d III, while *Xho* I were in reverse primers except to Fads2 where it was *Eco*R I.

Transcript	Step	Direction	Primer sequence	Temperature in °C (duration in sec.)				Enzyme
				Denaturation	Annealing	Extension	Cycles	
Fads2	First fragment	F	5'-TACACCTGGGAGGAGGTGCAG-3'	95 (30)	62.8 (90)	72 (60)	35	GoTaq
		R	5'-TGTCCGCTGAACCAGTCGTTGAA-3'					
	3' RACE first	F	5'-GAGCCAGTGGGTGAAGAGAC-3'	95 (30)	59 (30)	72 (150)	35	GoTaq
	3' RACE nested	F	5'- GAGCCACATCCCCATGAACA-3'	95 (30)	57 (30)	72 (150)	35	
	ORF cloning first	F	5'-GCAGCATTCAGAGTTTGATCAGCG-3'	95 (30)	61 (30)	72 (195)	35	Pfu
		R	5'-CCTCAATCGAGAAGCAATCAGAGC-3'					
	ORF cloning nested	F	5'-CCCGGATCCACGATGGGCGGC-3'	95 (30)	61 (30)	72 (195)	35	Pfu
		R	5'-CCGGAATCCTTATTTGTTGAGGTACG-3'					
	qPCR	F	5'-GAACTCTGGCTGGATGCGTA-3'	95 (15)	58.5 (30)	72 (30)	35	HiGreen
		R	5'-TCGTGGCACTTTGAATGTGT-3'					
Elovl2	First fragment	F	**5'**-GAGAGGATGGCTGCTGCTGGA-3'	95 (30)	60 (30)	72 (120)	35	GoTaq
		R	**5'**-GGCCCAAAGAAACTCTGTCCACA-3'					

	3’ RACE first	F	5’-CCGTCTTCATTGTGCTAAGGA-3’	95 (30)	57 (30)	72 (90)	35	GoTaq
	3’ RACE nested	F	5’-TCAGTTTCCTGCATGTGTATCAT-3’					
	5’ RACE first	R	5’-ACGGTAACCTGCAGACCAGA-3’	95 (30)	57 (30)	72 (90)	35	GoTaq
	5’ RACE nested	R	5’-GTTGGTGTGTAGGAATCCAGCA-3’					
	ORF cloning first	F	5’- CCAGCTGTCCCGTATTGTTTAACGG-3’	95 (30)	61 (30)	72 (195)	35	Pfu
		R	5’- CCATTCTATTGTTCATGTCGCGGC-3’					
	ORF cloning nested	F	5’- CCCGGATCCAATATGAACCAATTTG-3’	95 (30)	61 (30)	72 (195)	35	Pfu
		R	5’- CCGCTCGAGTCACTGCAGCTTC-3’					
	qPCR	F	5’-GGGTGGCAGAATGGCTAAGG-3’	95 (15)	58.5 (30)	72 (30)	35	HiGreen
		R	5’-TGCTTATCAGATGATTGGCTGC-3’					
Elovl5	First fragment	F	5’-CYTGGATGGGACCCAGARATC-3’	95 (30)	60 (45)	72 (60)	35	GoTaq
		R	5’-CTGGAACATGGTCAGGACAAAC-3’					
	3’ RACE first	F	5’-GGTTCGTCATGAACTGGGTG-3’	95 (30)	57 (30)	72 (90)	35	GoTaq
	3’ RACE nested	F	5’-ATTACGGCCTCTCTGCCATC-3’					
	5’ RACE first	R	5’-GGAGTACGGCTGTCTGTGC-3’	95 (30)	57 (30)	72 (90)	35	GoTaq
	5’ RACE nested	R	5’-GGCCCCATCCACACAATCAG-3’					
	ORF cloning first	F	5’-CCGCACAGGACTGAGAGCTAAAG-3’	95 (30)	61 (30)	72 (195)	35	Pfu
		R	5’-CGATATCAATGACCGGACTG-3’					

	ORF cloning nested	F	5’-CCAAGCTTAAGATGGAGTCCATTAATCTC-3’	95 (30)	61 (30)	72 (195)	35	Pfu
		R	5’-CCGCTCGAGTCAATCTGAGCG-3’					
	qPCR	F	5’-GGTTTGATGAACGGCCACAC-3’	95 (15)	58.5 (30)	72 (30)	35	HiGreen
		R	5’-GGTGTGCAAACATGTGAGGAG-3’					
β-actin	qPCR	F	5’-TGTGGGAGATGAGGCTCAGA-3’	95 (15)	58.5 (30)	72 (30)	35	HiGreen
		R	5’-GCCTCTGTAAGCAGGACAGG-3’					
ef1α	qPCR	F	5’- GTCGAGATGCACCACGAGTC-3’	95 (15)	58.5 (30)	72 (30)	35	HiGreen
		R	5’- GGGTGGTTCAGGATGATGAC-3’					

806 F, forward primer; R, reverse primer. Numbers in parentheses are time in seconds.

807 **Table 3.** Substrate conversion of transgenic yeast (*Saccharomyces*
808 *cerevisiae*) transformed with the fatty acyl desaturase (Fads2) of
809 *Tinca tinca* grown in the presence of added substrate.

FA substrate	FA product	Conversion (%)	Activity
18:2n-6	18:3n-6	8.8	Δ6
18:3n-3	18:4n-3	36.5	Δ6
20:2n-6	20:3n-6	nd	Δ8
20:3n-3	20:4n-3	nd	Δ8
20:3n-6	20:4n-6	5.2	Δ5
20:4n-3	20:5n-3	12.4	Δ5
22:4n-6	22:5n-6	nd	Δ4
22:5n-3	22:6n-3	nd	Δ4

810 Results are expressed as a percentage of total fatty acid substrate
811 converted to desaturated product. nd, no detected.

812 **Table 4.** Substrate conversion of transgenic yeast
813 (*Saccharomyces cerevisiae*) transformed with the fatty acyl
814 elongases 5 and 2 (Elovl5 and Elovl2, respectively) of *Tinca*
815 *tinca* grown in presence of added substrate.

FA substrate	FA product	Accumulated conversion (%)	
		Elovl5	Elovl2
18:2n-6	20:2n-6	18.5	2.5
18:3n-3	20:3n-3	35.6	7.2
18:3n-6	20:3n-6	77.3	12.5
18:4n-3	20:4n-3	79.6	14.9
20:4n-6	22:4n-6	14.9	23.0
20:5n-3	22:5n-3	37.6	58.8
22:4n-6	24:4n-6	nd	12.4
22:5n-3	24:5n-3	1.0	18.3

816 Results are expressed as a percentage of total fatty acid substrate
817 converted to elongated product. Nd, no detected.

818 **Table 5.** Total lipid (mg lipid/mg cell protein, % wet weight of muscle), total fatty acids
819 (µg fatty acid/mg cell protein, mg fatty acid/100g wet weight of muscle) and main fatty
820 acid composition (% of total fatty acids) of enterocytes, hepatocytes and muscle from
821 *Tinca tinca*.

	ENTEROCYTES	HEPATOCYTES	MUSCLE
Total lipid	0.3 ± 0.2	0.9 ± 0.3	1.4 ± 0.2
Total FA	48.6±23.8	252.7 ±84.7	985.8 ±133.7
Fatty acid			
14:0	1.1 ± 0.2	0.7 ± 0.2	1.3 ± 0.2
16:0	17.0 ± 0.6	17.7 ± 0.9	16.9 ± 0.7
18:0	9.0 ± 0.7	5.3 ± 0.7	2.9 ± 0.7
Total saturates[1]	30.4 ± 1.6	25.3 ± 1.4	22.2 ± 1.3
16:1n-7	3.0 ± 0.4	6.7 ± 2.1	7.5 ± 1.0
18:1n-9	22.7 ± 1.3	29.0 ± 7.6	33.3 ± 2.4
18:1n-7	3.2 ± 0.4	4.5 ± 0.4	3.6 ± 0.3
20:1n-9	1.0 ± 0.1	1.7 ± 0.4	1.3 ± 0.1
Total monoenes[1]	32.8 ± 1.4	43.2 ±10.2	47.2 ± 3.3
18:2n-6	7.1 ± 0.7	6.4 ± 0.7	10.8 ± 0.8
18:3n-6	nd	nd	0.2 ± 0.1
20:3n-6	0.8 ± 0.5	1.5 ± 0.5	1.0 ± 0.2
20:4n-6	3.8 ± 0.4	2.4 ± 1.1	1.6 ± 0.5
22:5n-6	0.6 ± 0.3	0.6 ± 0.2	0.5 ± 0.1
Total n-6 PUFA[1]	12.6 ± 2.0	11.6 ± 2.5	14.5 ± 0.6
18:3n-3	1.0 ± 0.2	1.2 ± 0.1	1.8 ± 0.3
20:5n-3	2.6 ± 0.2	2.3 ± 1.3	2.1 ± 0.2
22:5n-3	1.6 ± 0.2	1.1 ± 0.2	0.4 ± 0.5
22:6n-3	13.9 ± 1.2	13.2 ± 5.3	8.7 ± 1.8
Total n-3 PUFA[1]	19.2 ± 1.2	18.3 ± 7.0	13.7 ± 2.1
n-3/n-6	1.5 ± 0.2	1.5 ± 0.3	0.9 ± 0.1
Total n-3 LC-PUFA	18.1 ± 1.2	17.2 ± 6.9	11.5 ± 2.3

822 Results are presented as mean ± SD (n=5). Nd, no detected. [1] Includes other minor
823 components not shown.

824 **Table 6a.** Incorporation of radioactivity into total lipid (pmol mg prot^{-1} h^{-1}) and transformation (% of total radioactivity incorporated) obtained

825 from the in vivo incubation of enterocytes and hepatocytes from *Tinca tinca* with different [1-^{14}C] fatty acid substrates.

	ENTEROCYTES			HEPATOCYTES		
	18:2n-6	18:3n-3	20:5n-3	18:2n-6	18:3n-3	20:5n-3
Incorporation	61.3 ± 26.3	55.1 ± 34.6	49.2 ± 15.6	71.1 ± 13.8	61.5 ± 32.1	74.9 ± 43.2
FA recovery	84.6 ± 1.6 b	84.5 ± 3.5 b	74.4 ± 2.5 a	90.8 ± 1.4 b	93.7 ± 2.5 b	74.3 ± 3.6 a
Elongation	6.9 ± 1.2 a	8.8 ± 2.2 a	24.2 ± 2.2 b	1.0 ± 0.5	nd	25.3 ± 3.2
Desaturation	0.6 ± 0.4	1.1 ± 0.5	nd	1.1 ± 0.4	3.3 ± 1.5	nd
E+D	4.5 ± 0.6	5.4 ± 2.2	nd	6.0 ± 1.3	3.0 ± 1.7	nd
De novo	3.3 ± 0.7	nd	nd	1.1 ± 0.2	nd	nd
Unknown	0.2 ± 0.2	0.2 ± 0.2	1.4 ± 0.9	nd	nd	0.5 ± 0.7

826 Values are presented as mean ± SD (n=5). FA recovery, unmodified substrate; E+D, elongation and desaturation. Nd, no detected. Different

827 letters denote significant differences between [1-^{14}C] FA within each cell type ($P<0.05$).

828 **Table 6b.** Recovery of radioactivity (%) from [1-^{14}C] fatty

829 acid obtained from the *in vivo* incubation of enterocytes and

830 hepatocytes from *Tinca tinca*

	ENTEROCYTES	HEPATOCYTES
[1-^{14}C]*18:2n-6*		
18:2n-6	84.6 ± 1.6	90.8 ± 1.4
20:2n-6	4.9 ± 0.9	1.0 ± 0.5
18:3n-6	0.6 ± 0.4	1.1 ± 0.4
22:2n-6	1.2 ± 0.3	nd
24:2n-6	0.8 ± 0.2	nd
20:3n-6	1.1 ± 0.5	0.7 ± 0.3
22:3n-6	0.6 ± 0.7	2.7 ± 0.7
20:4n-6	1.1 ± 0.2	0.8 ± 0.2
22:5n-6	1.3 ± 0.7	1.2 ± 0.4
24:5n-6	0.4 ± 0.1	0.6 ± 0.2
[1-^{14}C]*18:3n-3*		
18:3n-3	84.5 ± 3.5	93.7 ± 2.5
20:3n-3	8.8 ± 2.2	nd
18:4n-3	1.1 ± 0.5	3.3 ± 1.5
20:4n-3	2.0 ± 1.0	2.3 ± 1.5
22:4n-3	1.2 ± 0.3	nd
20:5n-3	0.7 ± 0.4	0.5 ± 0.8
22:5n-3	0.6 ± 0.2	nd
22:6n-3	0.6 ± 0.2	0.2 ± 0.4
24:6n-3	0.3 ± 0.3	nd
[1-^{14}C]*20:5n-3*		
20:5n-3	74.4 ± 2.5	74.3 ± 3.6
22:5n-3	15.1 ± 1.6	15.3 ± 1.3
24:5n-3	2.9 ± 0.4	3.7 ± 1.1
26:5n-3	4.0 ± 0.6	3.9 ± 0.6
28:5n-3	2.3 ± 0.3	2.3 ± 0.4

831 Values are presented as mean ± SD (n=5).

832 **Figure legend**

833

834 **Figure 1.** Long chain fatty acids biosynthetic pathways from the precursors linoleic acid
835 and α-linolenic acid in teleosts.

836 **Figure 2.** Phylogenetic tree of *fads2* using the deduced amino acid sequences from
837 tench (*Tinca tinca*). The horizontal branch length is proportional to the amino acid
838 substitution rate per site. Demonstrate desaturase activities are included in all Fads-like
839 sequence as "Δx".

840 **Figure 3.** Phylogenetic tree of *elovl2* and *elovl5* using the deduced amino acid
841 sequences from tench (*Tinca tinca*). The horizontal branch length is proportional to the
842 amino acid substitution rate per site.

843 **Figure 4.** Tissue distribution of *fads2*, *elovl2* and *elovl5* from tench (*Tinca tinca*). Data
844 are presented as geometric mean log normalised expression ratios ± standard errors
845 (n=4, except for *fads2* where n=3). Different letters denote significant differences
846 among tissue for each gene.

847 **Figure 5.** Principal component analysis (PCA) of fatty acids (% of total fatty acids)
848 from enterocytes, hepatocytes, muscle of tench (*Tinca tinca*) and its diet. (A) Factor
849 loading plot for principal component 1 (PC1) and principal component 2 (PC2) (B)
850 Factor score plot.

851

852

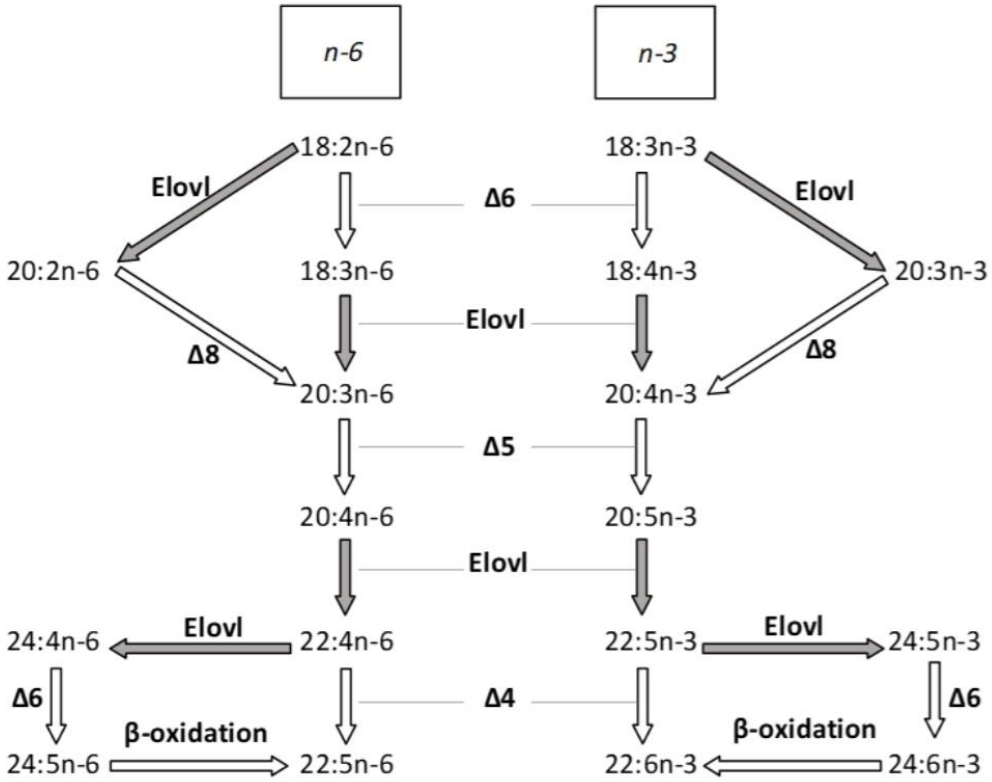

853

854

855

856

857

858

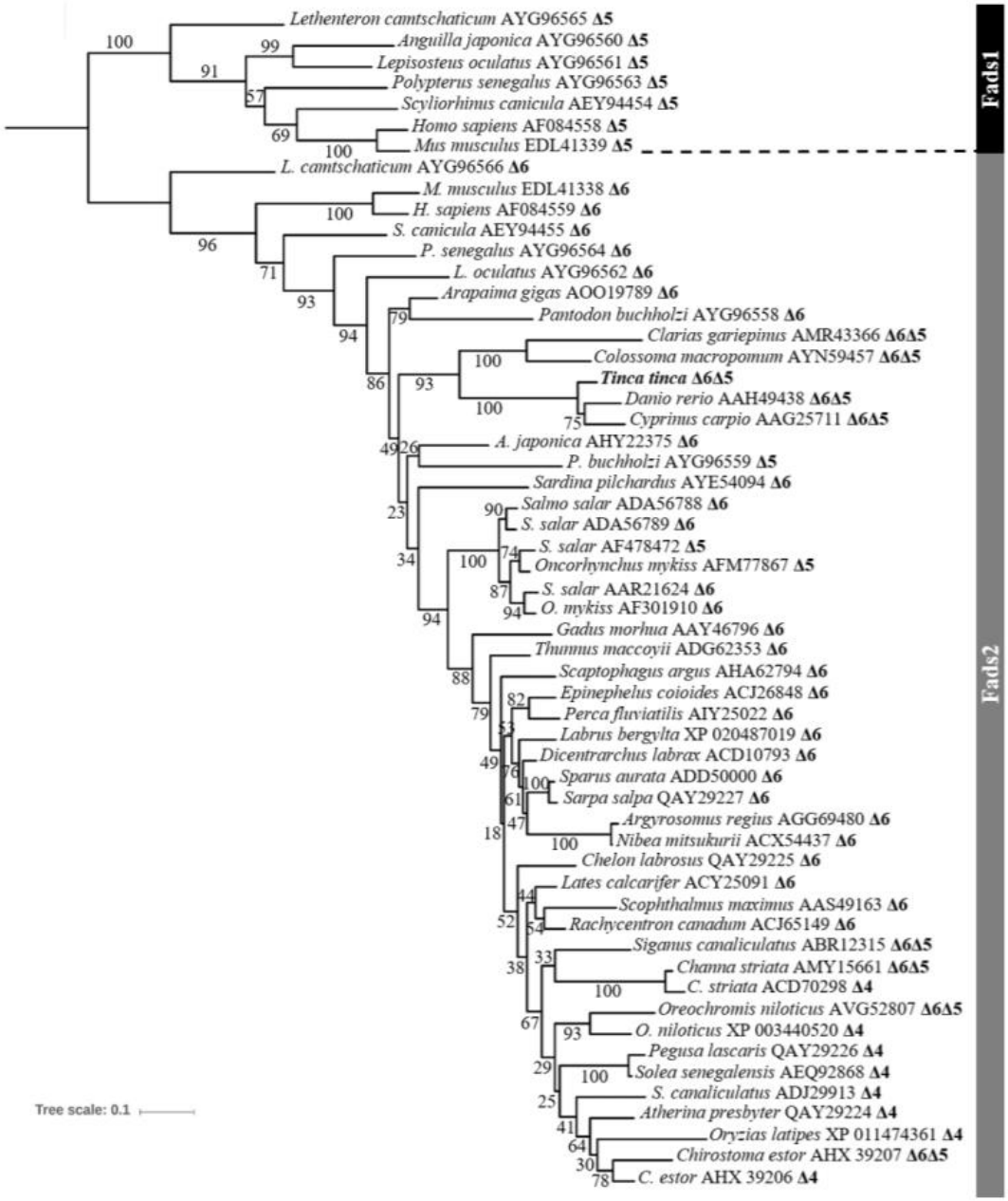

859

860

861

862

863

864

865

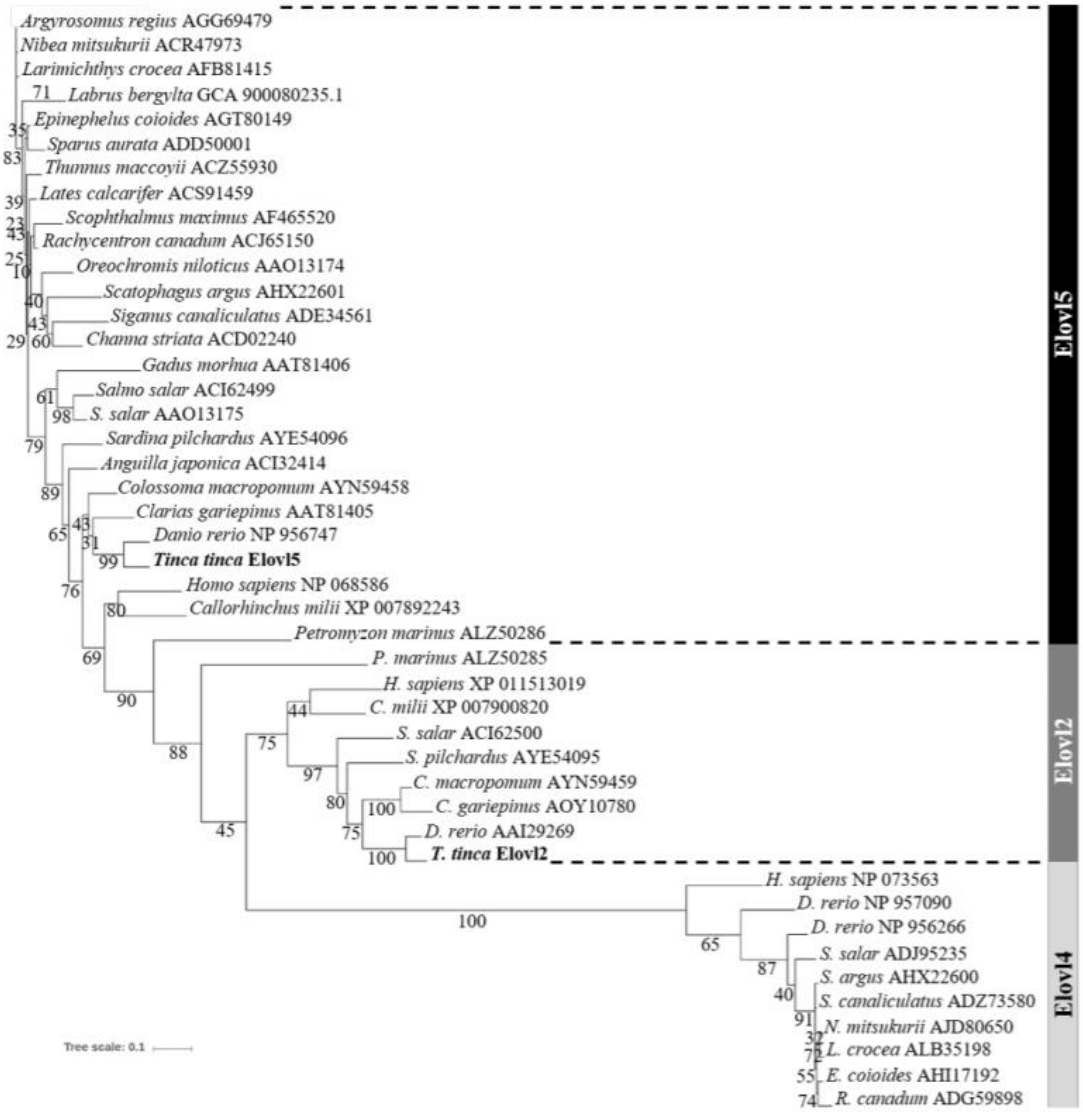
Argyrosomus regius AGG69479
Nibea mitsukurii ACR47973
Larimichthys crocea AFB81415
Labrus bergylta GCA 900080235.1
Epinephelus coioides AGT80149
Sparus aurata ADD50001
Thunnus maccoyii ACZ55930
Lates calcarifer ACS91459
Scophthalmus maximus AF465520
Rachycentron canadum ACJ65150
Oreochromis niloticus AAO13174
Scatophagus argus AHX22601
Sigamus canaliculatus ADE34561
Channa striata ACD02240
Gadus morhua AAT81406
Salmo salar ACI62499
S. salar AAO13175
Sardina pilchardus AYE54096
Anguilla japonica ACI32414
Colossoma macropomum AYN59458
Clarias gariepinus AAT81405
Danio rerio NP 956747
Tinca tinca Elovl5
Homo sapiens NP 068586
Callorhinchus milii XP 007892243
Petromyzon marinus ALZ50286
P. marinus ALZ50285
H. sapiens XP 011513019
C. milii XP 007900820
S. salar ACI62500
S. pilchardus AYE54095
C. macropomum AYN59459
C. gariepinus AOY10780
D. rerio AAI29269
T. tinca Elovl2
H. sapiens NP 073563
D. rerio NP 957090
D. rerio NP 956266
S. salar ADJ95235
S. argus AHX22600
S. canaliculatus ADZ73580
N. mitsukurii AJD80650
L. crocea ALB35198
E. coioides AHI17192
R. canadum ADG59898
Elovl5
Elovl2
Elovl4
Tree scale: 0.1

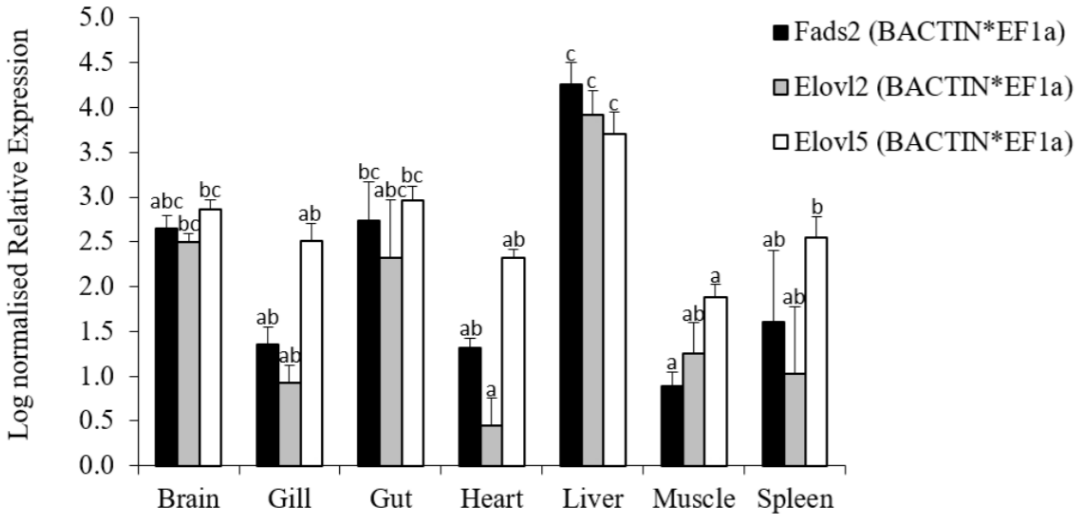

874

875

876

877

878

879

880

881

882

883

884

885

886

887

888

889

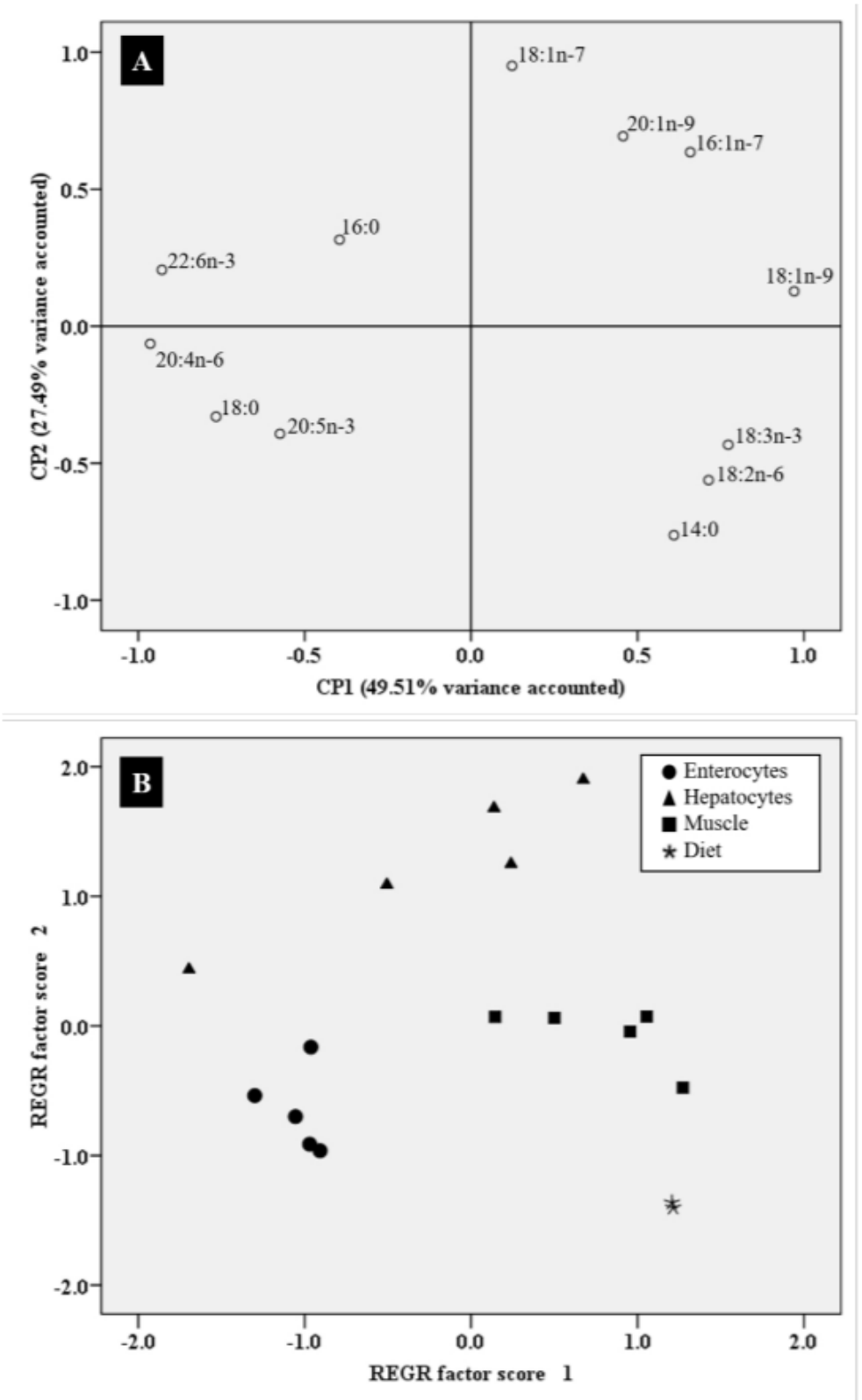
A
18:1n-7
20:1n-9
16:1n-7
16:0
22:6n-3
18:1n-9
20:4n-6
18:0
20:5n-3
18:3n-3
18:2n-6
14:0
CP2 (27.49% variance accounted)
CP1 (49.51% variance accounted)
B
Enterocytes
Hepatocytes
Muscle
Diet
REGR factor score 2
REGR factor score 1

890

891

892